Emma Keel, Marco Caffio, Des Gibson, and Carlos Garcia Nunez "Potential broadband photodetector concept based on three-dimensional graphene foam", Proc. SPIE 13015, Photosensitive Materials and their Applications III, 1301513 (18 June 2024); https://doi.org/10.1117/12.3017247

Potential Broadband photodetector concept based on three-dimensional graphene foam.

Emma Keel*[a], Marco Caffio[b], Des Gibson[a,c], Carlos Garcia Nunez[d]

[a] Institute of Thin Films, Sensors and Imaging, University of the West of Scotland, Paisley PA1 2BE, Scotland, UK
[b] Integrated Graphene Ltd., Stirling FK8 2DJ, Scotland, UK
[c] Albasense Ltd, Paisley PA1 2BE, Scotland, UK
[d] Electronics and Nanoscale Engineering, University of Glasgow, Glasgow G12 8QQ, Scotland, UK

** Contact author at: Institute of Thin Films, Sensors and Imaging, University of the West of Scotland, Paisley PA1 2BE, Scotland, UK*
e-mail address: emma.keel@uws.ac.uk

ABSTRACT

In this work, optical and structural properties of three-dimensional graphene (Gii™) foam have been analysed to validate the potential of this material as an active layer in broadband optoelectronic devices. The chemical structure of Gii™ foam was characterized by Raman spectroscopy carried out at different wavelengths (455, 532, 644, and 780 nm) and laser powers (1-8 mW). In this study, two types of Gii™ foam were analysed, including standard graphene (ST-Gii), and low resistance graphene (LR-Gii) whose main difference is the defects density modulating their electric conductivity. The performance of both ST-Gii and LR-Gii was determined by examining intensity and position, of G, D, and 2D peaks as a function of light source conditions (i.e., wavelength and power). Results demonstrate that ST-Gii presents a 1.37 G/D intensity ratio, which is 0.2 lower than that observed in LR-Gii, evidencing the drastic change in the electronic properties of both materials obtained during the synthesis process. Moreover, the study of the materials as a function of the wavelength showed – in the case of ST-Gii material – a clear 'optical switch' behaviour from G/D of 1.37 to 0.79 when the material is irradiated with light below and above 532nm, respectively. This interesting result indicates that Gii™ could be a potential candidate for optoelectronic devices (phototransistors, photodiodes, and photodetectors), thanks to the modulation of its electronic properties by irradiating the material to different light wavelengths. To further investigate this effect, in this work, we present the concept of a photo-resistive detector based on ST-Gii.

Keywords: photodetector, photo response, graphene, Raman spectroscopy, Optoelectronics

INTRODUCTION

Graphene foam is a solid, open-cell foam made of single-layer sheets of graphene and is a potential starting material for many engineering, energy, photonic and environmental applications due to its desirable mechanical properties, high specific area, and superior electrical transfer ability. Applications include wearable electronics,[1], [2], [3], energy storage devices,[4], [5] and sensors,[6], [7] thermal management [8], [9], [10] and other applications[11], [12]. The three-dimensional standard graphene foam, 3DST GiiTM (STG) and low resistance graphene foam 3DLR GiiTM (LRG) used in this work are materials grown using a patented process at Integrated Graphene Ltd Gii material, registered by Integrated Graphene Ltd., (2016). [13] Specific application focus in this work is a broadband photodetector.

The primary technique used in this investigation of graphene foam as a broadband detector is Raman spectroscopy. This is a non-destructive technique used to analysis materials by observing the inelastic scattered light that is characteristic in a molecular environment from the monochromatic light and a laser ranging from near ultraviolet to near infrared. [14], [15], [16] For Raman scattering there are two possible outcomes, the scattered light is either higher (anti stokes) or lower (stokes)

in energy than the incident light. [17], [18] The laser interacts with molecular vibrations causing the energy of the laser photons to be shifted up or down. The shift in energy gives information about the vibrational modes in the system.[15] Described in this paper we demonstrate through Raman spectroscopy an optical switch behaviour with the standard graphene foam material showing the potential for the material to be used as a broadband photodetector with a wavelength measured range from 455-780nm. Graphene is the classic material to be used with its high optical and electronic properties.[19]

Raman Spectroscopy is a powerful tool that can be used to characterise carbon-based materials. Carbon based materials have a unique feature being able to have a wide range of properties such as hardness, high porosity and electrical conductivity making graphene an appealing material that can be used over a range of applications. [20], [21] Raman spectroscopy specifically looks at the D and G peaks produced from the Raman spectrum. Where the D peak specifies the disorder in the material [22]and the G peak evaluates how much graphite is present in the material.[23] In this work we evaluate the characteristics of the D and G peaks present in the standard graphene and low resistance graphene foams, through conducting Raman spectroscopy over the visible and near infrared spectrum over a range of powers to test if there is a possibility for the standard or low resistance graphene foam to be used as a potential candidate for a broadband photodetector.

METHODOLOGY

Characterization using Raman spectroscopy utilises, 4mm diameter circular STG and LRG foams are deposited onto a 125-µm thick Kapton polyimide (PI) flexible substrate (Kapton® HN from UK insulations Ltd). The Raman spectroscopy was conducted using a Thermo Scientific DXR Raman microscope see figure 1 below. Before using, the system was set up correctly ensuring the laser used had the matching grating and filter installed. Once these are checked the machine is powered on and the laser key is switched on. The system had to be realigned and calibrated for each laser wavelengths used. The alignment is the process of bringing the laser beam and spectrograph sampling point into agreement along with the visual crosshair which selects the sampling point. The calibration assures the accuracy of the spectrum wavelength of the x and y axis.

Figure 1: Thermo Scientific DXR Raman Microscope

After the configurations take place, the sample is placed onto a glass microscope slide one at a time and loaded onto the microscope stage inside. Once secure the sample is centred and focused with a 10x objective. Now that the sample is focused the objective is changed to x50 and refocused to allow for better readings. The material is focused at x10 first, as it can be difficult to focus the sample at 50x without damaging the material. For each sample run the experiment has the same set-up with an aperture of 50µm pinhole and Raman shift range of 1000-3000cm^{-1} with the only change being the power and objective when need be. After the parameters have all been checked and approved the data for the sample is collected. The spectrum for all the samples produced show the Raman shift (cm^{-1}) along the x-axis with Intensity (cps) along the y-axis. The data is then saved as a .SPA and .CVS to be analysed. The same set-up for each sample takes place. In this paper we measure the standard graphene and low resistance graphene foams using a range of lasers wavelengths

across the spectrum; 455nm, 532nm, 663nm and 780nm at different powers 1-8mW at an objective of 50x to observe the difference in spectrum for D, G and 2D peaks.

RESULTS AND DISCUSSION

Figure 2 below shows how a typical graphene spectrum of Raman shift versus Intensity contains 3 main peaks, D, G and 2D peaks. Each of these peaks are affected by the excitation wavelength from the given laser being used, here it was a 532nm laser. The D and G peaks are in the first order Raman spectrum representing the disorder and how present the graphite signature of carbon is respectively, the higher the peak the more present it is. The 2D peak is part of the second order Raman spectrum, this peak is also sometimes known at G' as it is the second harmonic of the phonon density around the region of 1360 cm^{-1}. [23] In figure 2 the G peak is at a higher intensity than that of the D peak meaning the standard graphene is more carbon based with less defects present in the material. Table 1 below shows the range of values peak values found in figure 2.

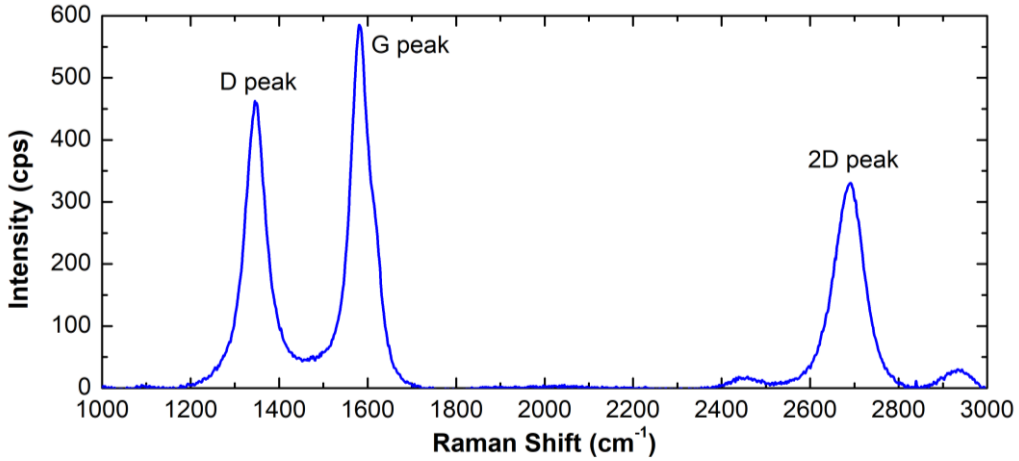

Figure 2: Example of the different peaks on a Raman spectrum for graphene, 532nm at 8mW.

Table 1 shows the maximum values in the Raman spectrum for the peak positions and intensities at each power measurement ranging from 1mW-8mW. The common range for graphene materials to have their peaks are approximately D peak (1300-1400 cm^{-1}), G peak (1500-1600 cm^{-1}) and 2D peak (2600-2700cm^{-1}). From the results below it can be seen that all the peak positions fall within the category. The table shows that as the power is increased, the intensity (counts per second, cps) of all the peaks increases due to the higher excitation wavelength given from the power.

Table 1: 532nm Raman spectra data at the peak positions over a range of powers for standard graphene foam.

Power (mW)	D peak position (cm^{-1})	Intensity (cps)	G peak position (cm^{-1})	Intensity (cps)	2D peak position (cm^{-1})	Intensity (cps)
1	1348.288	81.922	1587.418	98.696	2695.322	57.4520
2	1350.216	184.012	1584.525	223.898	2692.429	128.514
3	1349.252	297.290	1582.596	363.660	2694.357	222.913
4	1346.359	396.190	1584.525	494.800	2691.465	284.365
5	1345.395	462.369	1580.668	585.345	2691.465	330.618
6	1347.323	547.399	1580.668	715.256	2682.787	419.368
7	1342.502	619.027	1579.704	814.596	2681.822	453.905
8	1344.431	702.095	1579.704	959.324	2680.858	518.402

A study was conducted to see how the standard graphene foams peak intensities varied with power. The power measurements were taken in the mW range as when a high-powered laser is irritated onto a carbon-based sample it can affect the temperature of the material and change and/or damage the surface of the material. In figure 3 below the three

different figures represent each specific peak in the standard graphene spectrum over a range of laser wavelengths. Across all three figures the optimal wavelength for the STG material is 532nm, this is due to there being low fluorescence background for carbon-based materials at approximately 500nm. [16] From figure 3(a) and figure 3(c) the D peaks are related showing the same intensity peaks being higher at 633nm than 455nm, this means there are a higher count of defects present in the material compared to 455nm which shows a higher value of graphite in the G peak position figure 3(b).

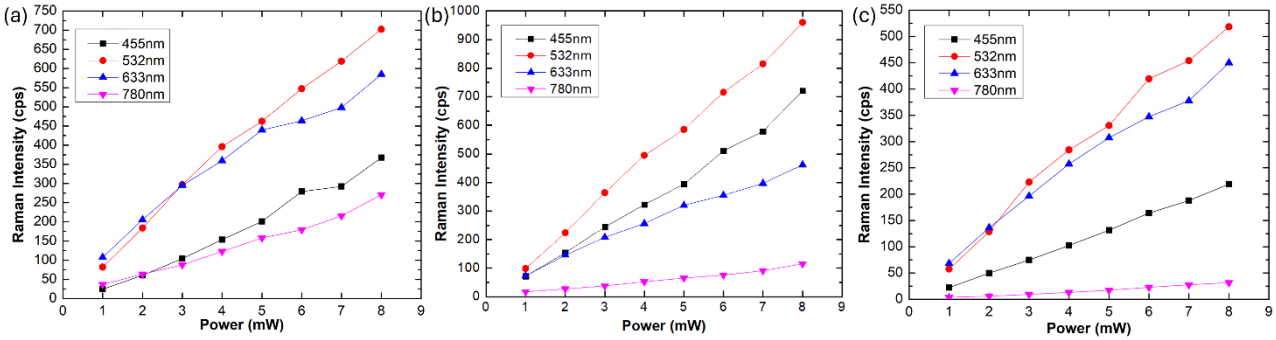

Figure 3: Comparison of Intensity vs Power for (a) D peak position, (b) G peak position, (c) 2D peak position for all laser wavelengths.

Figure 4 below shows a comparison of the low resistance and standard graphene foams using an excitation wavelength of 532nm at 8mW. One of the main differences between the materials is their structure, the standard graphene material has a more porous structure whereas the low resistance graphene is more compact meaning there is less space for particles to move. Due to the LRG foam having low resistance this means the electrical conductivity of the material is greater than the STG foam. This happens due to the confinement and reduces dimensionality affecting the materials properties.[24] The higher conductivity for the LRG is shown in figure 4 below, where the intensity (cps) is higher at all peaks present in the material.

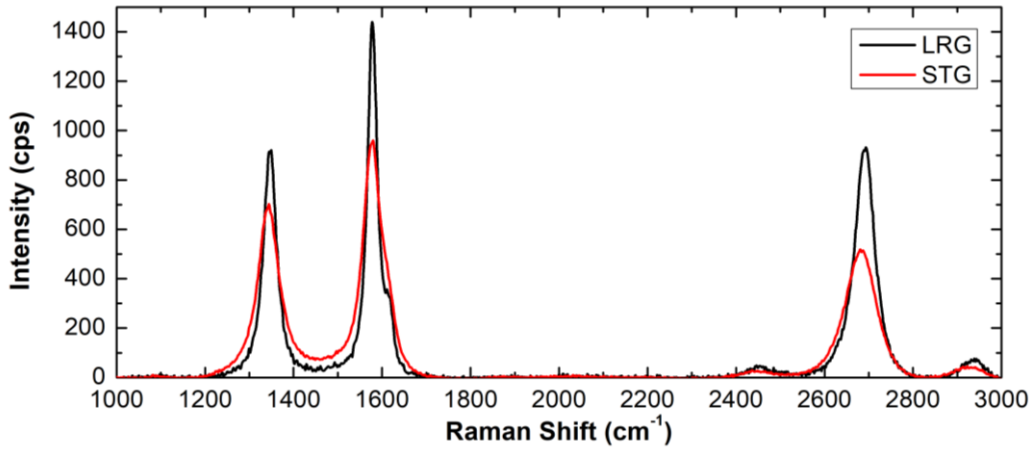

Figure 4: Comparison of peaks for low resistance graphene (LRG) and standard graphene (STG) foam at 532nm 8mW.

The results in figure 4 shows that the STG presents a 1.37 G/D intensity ratio, which is 0.2 lower than that observed in LRG exhibiting a more drastic change in the electronic properties of both materials obtained during the synthesis process.

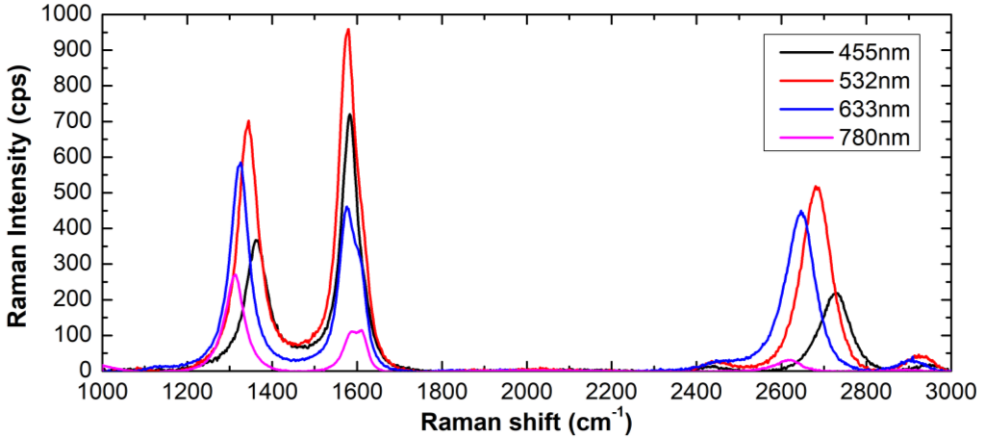

Figure 5: Raman spectra comparison of laser wavelengths with standard graphene (STG) foam at 8 mW.

Figure 5 shows the comparison of all four excitation wavelengths measured at 8mW for the standard graphene foam. Bringing together the information extracted from figures 3 and 4 the optical excitation wavelength to use for graphene is 532nm as it produces the more prominent peak values for the D, G, and 2D peak due to the fluorescence background being lowest at this excitation wavelength. In figure 5 the STG foam as a function of the excitation wavelengths shows a clear 'optical switch' behaviour happening from G/D of 1.37 to 0.79 when the material is irradiated with light below and above 532nm, respectively. In the first investigation of the Raman spectrum in graphite, Tuinstra and Koenig [25] related the D peak as the zone-centre phonon mode which is seen in single crystalline graphite but isn't Raman active. [22] Whereas polycrystalline materials like standard graphene foam have disorder in their materials to allow them to be Raman active. It is known that the D peak is in the phonon density of sate distribution meaning the photon energy varies with the excitation wavelength used. When we look closely at figure 5 specifically the D peak values for all the excitation wavelengths, shown in figure 6 more clearly.

In figure 6 a dispersion of the D peak is shown through the Raman shift. The measurements taken by I. Pócsik [22] shows that resonant scattering occurs when the phonons present have the same k-vector as the photon responsible for the resonance and the G peak showed no indication of changing with the excitation wavelength but done so with the D peak specifically with frequency and intensity.

Figure 6 shows the four excitation wavelengths in relation to Raman shift versus intensity. It is seen that the D peak value shifts depending on the excitation wavelength, at 780nm the Raman shift sits at 1313.7cm^{-1} increasing to 1362.2cm^{-1} at 455nm. This is due to different excitation energies being produced for the different wavelengths with 780nm producing the smallest excitation wavelength and 455nm producing the highest excitation wavelength.

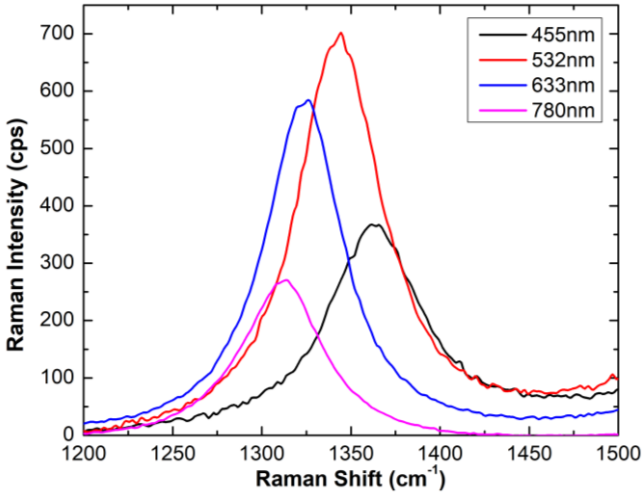

Figure 6: Comparison of the D peak for the four excitation wavelengths.

CONCLUSION

This work demonstrates through Raman spectroscopy the potential for the standard graphene foam to be used as an active layer in broadband optoelectronic devices. The two materials were examined by looking at the D, G and 2D peaks at different excitation energies 455, 532, 633 and 780nm and laser powers ranging from 1-8mW. When comparing the two materials STG and LRG foam it can be seen the main differences of the materials were the number of defect present in the material alongside the electrical conductivity. The results showed that the STG foam presented a ratio of 1.37 which was lower than the LRG foam at 532nm. The specific STG presented an optical switch behaviour in the D peak when all four Raman spectrums of each excitation wavelength were compared showing the D/G ratio to change from 1.37 at 532nm to 0.79nm at the wavelengths above and below 532nm as well as the excitation wavelength of the D peak showing the potential conversion of photons into phonons resonance. This interesting result shows the potential of the STG foam being used as a broadband photodetector. Future work will investigate the STG foam as a broadband photodetector using a light source combined with a liner variable filter to enable detection over the visible and infrared reigns.

ACKNOWLEDGEMENTS

The authors are grateful for financial support from Scottish Research Partnership in Engineering (NMIS/IDP-011) and British Council & Higher Education Commission (20-ICRG-165/RGM/HEC/2020), Integrated Graphene limited and the University of the West of Scotland.

REFERENCES

[1] Y. Meng *et al.*, 'All-graphene core-sheath microfibers for all-solid-state, stretchable fibriform supercapacitors and wearable electronic textiles', *Advanced materials*, vol. 16, no. 25, pp. 2326–2331, 2013.

[2] Y. Wang *et al.*, 'Wearable and highly sensitive graphene strain sensors for human motion monitoring', *Adv Funct Mater*, vol. 24, no. 29, pp. 4666–4670, 2014.

[3] K. P. Bera *et al.*, 'Trapped Photons Induced Ultrahigh External Quantum Efficiency and Photoresponsivity in Hybrid Graphene/Metal-Organic Framework Broadband Wearable Photodetectors', *Adv Funct Mater*, vol. 28, no. 51, p. 1804802, 2018.

[4] C. T. Phare, Y.-H. Daniel Lee, J. Cardenas, and M. Lipson, 'Graphene electro-optic modulator with 30 GHz bandwidth', *Nat Photonics*, vol. 9, no. 8, pp. 511–514, 2015.

[5] O. Balci *et al.*, 'Electrically switchable metadevices via graphene', *Sci Adv*, vol. 4, no. 1, p. eaao1749, 2018.

[6] J. Yun *et al.*, 'Stretchable patterned graphene gas sensor driven by integrated micro-supercapacitor array', *Nano Energy*, vol. 19, pp. 401–414, 2016.

[7] S. Goossens *et al.*, 'Broadband image sensor array based on graphene–CMOS integration', *Nat Photonics*, vol. 11, no. 6, pp. 366–371, 2017.

[8] P. B. Pawar, S. Saxena, D. K. Badhe, R. P. Chaudhary, and S. Shukla, '3D oxidized graphene frameworks for efficient nano sieving', *Sci Rep*, vol. 6, no. 1, p. 21150, 2016.

[9] S. Ramirez *et al.*, 'Thermal and magnetic properties of nanostructured densified ferrimagnetic composites with graphene-graphite fillers', *Mater Des*, vol. 118, pp. 75–80, 2017.

[10] X. Hu *et al.*, 'Tailoring Graphene Oxide-Based Aerogels for Efficient Solar Steam Generation under One Sun.', *Adv Mater*, vol. 29, no. 5, 2016.

[11] Y. Zhang *et al.*, 'Broadband and tunable high-performance microwave absorption of an ultralight and highly compressible graphene foam', *Advanced materials*, vol. 27, no. 12, pp. 2049–2053, 2015.

[12] E. Keel *et al.*, 'Three-dimensional graphene foam based triboelectric nanogenerators for energy systems and autonomous sensors', *Nano Energy*, vol. 112, Jul. 2023, doi: 10.1016/j.nanoen.2023.108475.

[13] 'Gii material, registered by Integrated Graphene Ltd., (2016). https://www. integratedgraphene.com/gii-technology (accessed February 23, 2023). '.

[14] R. S. Das and Y. K. Agrawal, 'Raman spectroscopy: Recent advancements, techniques and applications', *Vib Spectrosc*, vol. 57, no. 2, pp. 163–176, 2011.

[15] E. V Efremov, F. Ariese, and C. Gooijer, 'Achievements in resonance Raman spectroscopy: Review of a technique with a distinct analytical chemistry potential', *Anal Chim Acta*, vol. 606, no. 2, pp. 119–134, 2008.

[16] E. F. Antunes, A. O. Lobo, E. J. Corat, V. J. Trava-Airoldi, A. A. Martin, and C. Ver\'\issimo, 'Comparative study of first-and second-order Raman spectra of MWCNT at visible and infrared laser excitation', *Carbon N Y*, vol. 44, no. 11, pp. 2202–2211, 2006.
[17] L. Lin, X. Bi, Y. Gu, F. Wang, and J. Ye, 'Surface-enhanced Raman scattering nanotags for bioimaging', *J Appl Phys*, vol. 129, no. 19, 2021.
[18] T. H. Kauffmann, N. Kokanyan, and M. D. Fontana, 'Use of Stokes and anti-Stokes Raman scattering for new applications', *Journal of Raman Spectroscopy*, vol. 50, no. 3, pp. 418–424, 2019.
[19] T. Deng *et al.*, 'Three-dimensional graphene field-effect transistors as high-performance photodetectors', *Nano Lett*, vol. 19, no. 3, pp. 1494–1503, 2019.
[20] Y. Wang, D. C. Alsmeyer, and R. L. McCreery, 'Raman spectroscopy of carbon materials: structural basis of observed spectra', *Chemistry of Materials*, vol. 2, no. 5, pp. 557–563, 1990.
[21] J. R. Dennison, M. Holtz, and G. Swain, 'Raman spectroscopy of carbon materials', *Spectroscopy*, vol. 11, no. 8, 1996.
[22] I. Pócsik, M. Hundhausen, M. Koós, and L. Ley, 'Origin of the D peak in the Raman spectrum of microcrystalline graphite', *J Non Cryst Solids*, vol. 227, pp. 1083–1086, 1998.
[23] Y. Kaburagi, A. Yoshida, and Y. Hishiyama, 'Raman spectroscopy', in *Materials Science and Engineering of Carbon*, Elsevier, 2016, pp. 125–152.
[24] C. Qiu, K. E. Bennet, T. Khan, J. D. Ciubuc, and F. S. Manciu, 'Raman and conductivity analysis of graphene for biomedical applications', *Materials*, vol. 9, no. 11, p. 897, 2016.
[25] F. Tuinstra and J. L. Koenig, 'Raman spectrum of graphite', *J Chem Phys*, vol. 53, no. 3, pp. 1126–1130, 1970.